Segregation of Block Copolymers to Interfaces between Immiscible Homopolymers

Kenneth R. Shull*,† and Edward J. Kramer

Department of Materials Science and Engineering, Cornell University, Ithaca, New York 14853

Georges Hadziioannou‡ and Wing Tang§

IBM Almaden Research Center, 650 Harry Road, San Jose, California 95120

Received December 15, 1989; Revised Manuscript Received April 19, 1990

ABSTRACT: The equilibrium segregation of deuterated polystyrene–poly(2-vinylpyridine) diblock copolymers to interfaces between high molecular weight polystyrene and poly(2-vinylpyridine) homopolymers was measured by forward recoil spectrometry. The dependence of the integrated segregation on the equilibrium copolymer concentration in the PS phase is compared to predictions from a mean-field theory in which the copolymer chemical potential is the relevant parameter. Predictions from the theory are quantitatively accurate for values of the copolymer chemical potential, which are below a certain limiting value associated with the formation of block copolymer micelles. The segregation behavior in the regime where micelles are present is complicated by a strong tendency for micelles to segregate to the free polystyrene surface and by a weaker tendency for micelles to segregate to the interfacial region. Values of the copolymer chemical potential at the micelle transition are obtained from a careful analysis of the data and are in reasonable agreement with predictions from a simplified theory of micelle formation.

Introduction

The behavior of phase-separated polymer systems is governed to a large extent by the interfacial properties. One important parameter is the interfacial tension, γ, which determines the thermodynamic stability of a curved interface. Small values of γ are desirable if an immiscible polymer blend is to consist of a dispersion of small second-phase particles in a continuous matrix phase. Rubber-toughened plastics are an example where such a dispersion is desirable. Impact toughness of these materials is enhanced by the inclusion of a dispersion of small rubber particles as a second phase, but only if there is good adhesion between the rubber particles and the glassy matrix phase.[1] The mechanical stability of the interface between immiscible polymers, determined by the specific molecular structure in the interfacial region, is therefore another important factor that must be considered in addition to the interfacial tension.

One method of producing mechanically stable, low-energy interfaces is to add small amounts of diblock copolymer to the phase-separated system. The block copolymer is designed such that each block has a preferential affinity for a different homopolymer, with the result that the copolymer segregates preferentially to the interface between homopolymers. The interfacial excess of copolymer is related to γ through the Gibbs adsorption equation. For dilute copolymer solutions terms involving the chemical potentials of the homopolymers can be ignored, giving

$$\gamma(\mu_c) = \gamma_0 - \int_{-\infty}^{\mu_c} \nu_i(\mu_c')\, d\mu_c' \qquad (1)$$

where ν_i is the interface excess of copolymer in chains per unit area, μ_c is the copolymer chemical potential, and γ_0 is the interfacial tension in the absence of block copolymer. A decrease in the interfacial tension of polymer mixtures in the presence of block copolymer has been observed experimentally.[2,3]

Block copolymers also increase the mechanical strength of an interface by increasing the number of molecular entanglements between the two phases. The width of the interface between strongly incompatible polymers is quite small, and very few entanglements will be formed in this region. When block copolymer is added to the system, the effective width of the interface is increased by the penetration of the blocks into the homopolymer phases.[4] More entanglements will be formed across this larger interfacial region, giving rise to an increased interfacial strength as has been verified by direct measurement[5] and by consideration of the mechanical properties of phase-separated blends in the presence of block copolymer.[6,7]

Segregation of block copolymer to homopolymer interfaces has been inferred from the results mentioned above and has been observed qualitatively by transmission electron microscopy.[8] Here we directly measure the amount of the equilibrium interfacial block copolymer segregation in a well-characterized model system consisting of diblock copolymers of deuterated polystyrene (dPS) and poly(2-vinylpyridine) (PVP) at interfaces between PS and PVP homopolymers.

Experimental Section

The chemical structures of PS, PVP, and dPS–PVP block copolymer are shown in Figure 1. We used high molecular weight homopolymers with degrees of polymerization $N_{h\text{-}ps}$ and $N_{h\text{-}pvp}$ equal to approximately 6000. These polymers had narrow molecular weight distributions, with $M_w/M_n < 1.1$ for the PS homopolymer and $M_w/M_n < 1.2$ for the PVP homopolymer. We refer to the copolymers by the number average degrees of polymerization of the dPS and PVP blocks, for example, 391–68, where 391 is $N_{c\text{-}dps}$, the degree of polymerization of the dPS block, and 68 is $N_{c\text{-}pvp}$, the degree of polymerization of the PVP block.

The block copolymers were synthesized via anionic polymerization in THF at temperatures between −55 and −65 °C, with cumyl potassium as the initiator. The reaction and all distillations were carried out under purified argon. The deuterated polystyrene block was polymerized first, and a small amount of this polymer was removed prior to the addition of vinylpyridine

† Current address: IBM Almaden Research Center, 650 Harry Road, San Jose, CA 95120.
‡ Current address: Department of Chemistry, University of Groningen, Nijenborgh 16, 9747 AG Groningen, The Netherlands.
§ Current address: IBM General Products Division, 5600 Cottle Road, San Jose, CA 95193.

0024-9297/90/2223-4780$02.50/0 © 1990 American Chemical Society

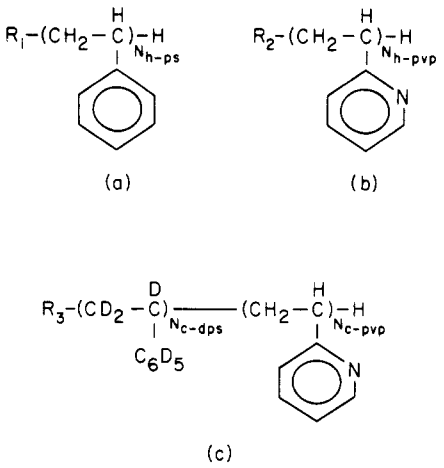

Figure 1. Chemical structures of the polymers used in this study: (a) polystyrene, (b) poly(2-vinylpyridine), (c) diblock copolymer of deuterated polystyrene and poly(2-vinylpyridine). Here, R_1, R_2, and R_3 are initiator fragments from the anionic polymerization, which are similar in size to the repeat units.

Table I
SEC Characterization of the Block Copolymers

$N_{c\text{-}dps}$–$N_{c\text{-}pvp}$	M_w/M_n (dPS block)	M_w/M_n (overall)
391–68	1.03	1.03
355–125	1.07	1.07
1300–173	1.04	1.07

monomer. The number-average degree of polymerization and polydispersity of the polystyrene precursor were measured by size-exclusion chromatography (SEC). Relative volume fractions of PVP and dPS in the copolymers were measured by forward recoil spectrometry (FRES).[9-11] The number-average degree of polymerization of the PVP block is given by

$$N_{c\text{-}pvp} = N_{c\text{-}dps}\left(\frac{\text{vol. fraction of PVP}}{\text{vol. fraction of dPS}}\right) \quad (2)$$

An estimate of the overall polydispersity of the block copolymers was obtained by SEC. These values are approximate, due to problems associated with adsorption of the block copolymer onto the chromatographic columns. The characteristics of the copolymers used are summarized in Table I.

Interfaces between thin films of PS and PVP homopolymers were created in the presence of dPS–PVP block copolymer. Two sample geometries were used in order to assess the importance of kinetic limitations associated with the formation of block copolymer micelles. In the constant-concentration geometry, shown in Figure 2a, copolymer diffuses toward the interface from an initially uniform concentration of copolymer chains and micelles in the PS layer. In the interface excess geometry, shown in Figure 2b, block copolymer diffuses away from an initial excess of block copolymer chains at the interface. Sufficiently long annealing times produce an interface excess of block copolymer chains in equilibrium with a uniform concentration of chains and micelles in the PS phase. If equilibrium with respect to the PS phase is truly attained, the final interfacial copolymer excess will depend only on the final copolymer concentration in the PS phase and not on the initial sample configuration.

All samples were prepared by first spin casting 2000 Å of the PVP homopolymer from a glacial acetic acid solution onto a polished silicon substrate. The uniform concentration samples were prepared by spin casting a 4000-Å layer of the PS homopolymer containing a small amount of copolymer directly onto the PVP layer from a toluene solution. The interface excess samples were prepared by spin casting a 600-Å film containing approximately 30% block copolymer onto the PVP layer. A 4000-Å layer of the PS homopolymer was then spun onto a glass slide, floated off onto a water bath, and picked up on top of the previous two layers. All samples were annealed in vacuo at 178 °C. The distributions of block copolymer in the samples were measured by depth profiling the deuterium in the block copolymer by FRES as described in previous publications.[9-11]

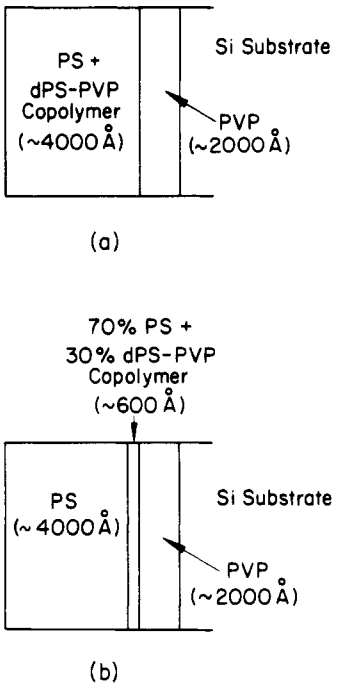

Figure 2. Two different sample geometries, showing the copolymer distributions prior to the annealing step: (a) constant concentration geometry, (b) interface excess geometry.

Results and Discussion

The formation of micelles in the polystyrene phase competes with the segregation to the interface, and an accurate interpretation of our results can only be obtained if the effects of micelle formation are understood. The PS–copolymer solutions from which the samples were cast did not contain micelles. These micelles form during the spin-casting process and during the subsequent high-temperature anneal. As described in Appendix 1, micelles form at lower values of the copolymer chemical potential, μ_c, when the smaller block forms the core rather than when the larger block forms the core. The copolymers used in this study have PVP blocks that are shorter than the corresponding dPS blocks, so micelles will form in the PS phase at lower values of μ_c than are necessary for the appearance of micelles in the PVP phase. The copolymer chemical potential increases as the volume fraction of copolymer in the PS phase, ϕ_c^{ps}, increases. Micelles appear in the PS phase when μ_c reaches the critical value, μ_{cmc}^{ps}, at which point $\phi_c^{ps} = \phi_{cmc}^{ps}$, the critical micelle concentration in the PS phase. Further increases in ϕ_c^{ps} increase the concentration of micelles in the system but do not lead to appreciable increases in μ_c or the concentration of free block copolymer chains.[12] The copolymer chemical potential remains pinned at values that are too low to lead to the formation of micelles in the PVP phase. As described in the next section, the solubility of free block copolymer chains at a given value of μ_c is an exponentially decreasing function of the molecular weight of the incompatible block. The copolymers that we have used have $N_{c\text{-}dps} \gg N_{c\text{-}pvp}$. For all reasonable values of μ_c, the solubility of the block copolymer chains in the PVP phase is therefore exceptionally low and can be neglected.

A typical copolymer distribution for an unannealed constant-concentration sample is shown in Figure 3. The broadening of the edges of the distribution arises from the convolution of the true distribution with the instrumental resolution function, a Gaussian with a full-width at half-maximum of 800 Å. The copolymer distribution for a constant-concentration sample of the 391–68 copolymer

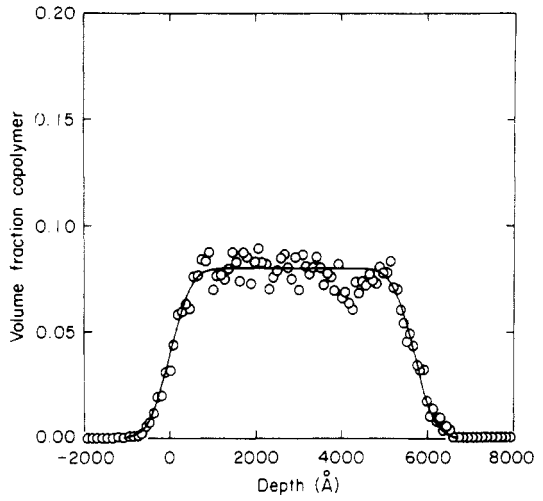

Figure 3. Copolymer distribution in a typical constant concentration sample prior to the annealing step.

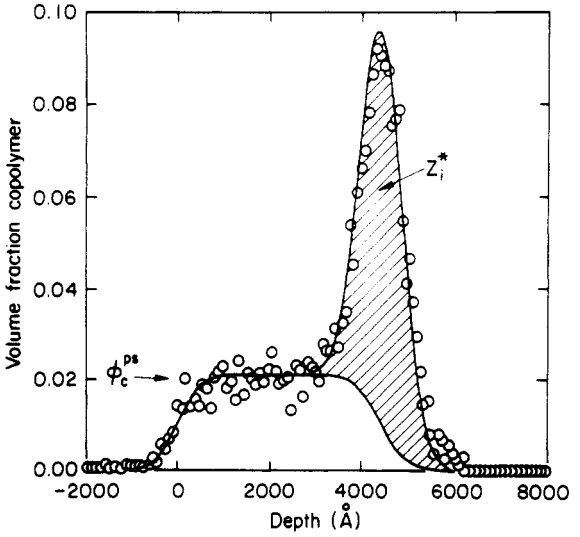

Figure 4. Copolymer distribution from a 391–68 constant-concentration sample after an 8-h anneal at 178 °C. For this sample ϕ_c^{ps}, the final equilibrium copolymer concentration in the PS phase, is 2.1%. The interface copolymer excess, z_i^*, corresponds to the hatched area and is equal to 100 Å.

after an 8-h anneal at 178 °C is shown in Figure 4. Interface excess samples give identical results, indicating that these annealing conditions give an equilibrated interface for this block copolymer. The samples with the 355–125 copolymer were also found to be in equilibrium, although annealing times of several days were required.

Because the depth resolution of FRES is not sufficient to resolve details within the segregated layer, we measure z_i^*, the total excess copolymer at the interface, corresponding to the hatched area in Figure 4 and defined as

$$z_i^* = \int_{-\infty}^{+\infty} dx\, (\phi_c(x) - \phi_c^{ps}) \qquad (3)$$

where ϕ_c is the local copolymer volume fraction and ϕ_c^{ps} is the copolymer volume fraction in the bulk PS phase in equilibrium with the segregated layer. The interfacial copolymer excess in chains/area, ν_i, is obtained from z_i^* by dividing by the copolymer molecular volume.

The volume fraction of copolymer in the PS phase in equilibrium with the segregated layer in Figure 4 is 2.1%. A very different situation occurs when the final equilibrium volume fraction is 5.8%, as shown in Figure 5. There is a large amount of copolymer that segregates to the free polystyrene surface, giving rise to a surface copolymer

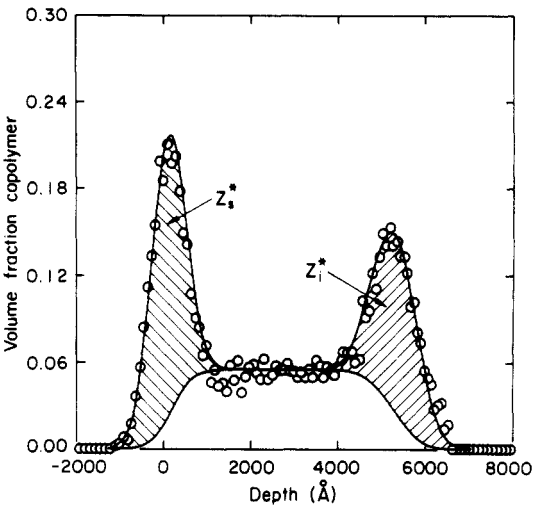

Figure 5. Copolymer distribution from a 391–68 constant-concentration sample after an 8-h anneal at 178 °C. The final equilibrium copolymer concentration in the PS phase is 5.8%, with z_i^* = 155 Å. There is also a surface copolymer excess, z_s^*, equal to 200 Å.

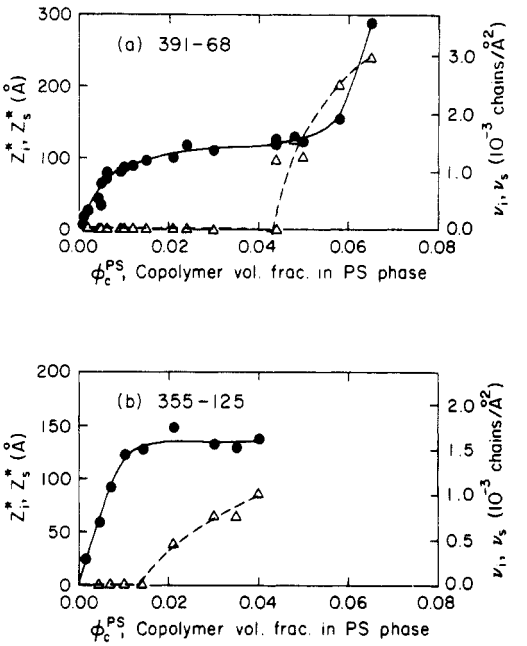

Figure 6. Interface (●—) and surface (△- - -) copolymer excesses as functions of the equilibrium copolymer volume fraction in the PS phase: (a) 391–68 copolymer, (b) 355–125 copolymer. The solid and dashed lines are aids to the eye, whereas the symbols represent the actual measured values.

excess, z_s^*, and the corresponding ν_s. Here z_s^* and z_i^* are defined by evaluating the integral in eq 3 in the vicinity of the appropriate segregated layer. In Figure 6a z_i^* and z_s^*, or alternatively ν_i and ν_s, for the 391–68 copolymer are plotted as functions of the equilibrium copolymer concentration in the PS phase. Similar plots for the 355–125 copolymer are shown in Figure 6b. Figure 7 shows the copolymer concentration profile for a uniform concentration sample of the 1300–173 copolymer after a 6-day anneal at 178 °C. The depleted regions adjacent to the segregated layers indicate that this sample is not fully equilibrated. The measured values of 210 Å for z_i^* and 74 Å for z_s^* are therefore only approximations to the true equilibrium values.

As illustrated by parts a and b of Figure 6, there is a critical value of ϕ_c^{ps} below which there is no surface copolymer excess. The existence of this transition indicates

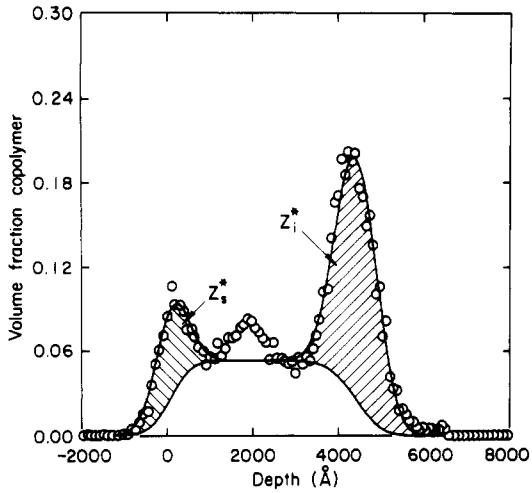

Figure 7. Copolymer distribution from a 1300–173 constant-concentration sample after a 6-day anneal at 178 °C. The depletion zones adjacent to the segregated layers indicate that the sample is not fully equilibrated. The hatched regions correspond to $z_i^* = 210$ Å and $z_s^* = 74$ Å and do not necessarily correspond to the equilibrium values of these quantities.

that segregation of individual copolymer chains to the surface does not account for the observed surface segregation. The onset of surface segregation at the critical value of ϕ_c^{ps} must instead be associated with the formation of an organized copolymer assembly that has an affinity for the free surface. The fact that individual copolymer chains do not segregate to the polystyrene surface is consistent with the expectation that the polar PVP has a higher surface tension that the nonpolar PS.

We attribute the appearance of the copolymer assembly at the surface to the surface segregation of block copolymer micelles. There are two potential driving forces for this surface segregation, the first being the tendency for the system to reduce the number of sharp interfaces that are present. The number of available polymer conformations in the presence of such an interface is sharply reduced, resulting in an increased free energy that is completely entropic in origin. The interface between the micellar corona and the surrounding high molecular weight homopolymer is similar in width to the homopolymer radius of gyration, and there will be a certain interfacial tension associated with this interface.[4] The overall free energy of the system can be reduced by placing the micelles at the free PS surface, thereby reducing the corona–homopolymer interfacial area.

A second driving force for the surface segregation of dPS–PVP block copolymer micelles arises from enthalpic interactions between normal and deuterated polystyrene. Isotopic blends of normal and deuterated molecules do not mix ideally but are influenced by the finite polarizability difference between C–H and C–D bonds.[13] This polarizability difference gives rise to an unfavorable interaction between the two species and to a slightly lower surface tension for the deuterated component. The resulting tendency for deuterated chains to segregate to a free surface is counterbalanced by the entropy of mixing. Surface segregation of the deuterated component has been observed in isotopic blends of high molecular weight polymers, where the entropy of mixing is quite low.[14] The PVP core of a dPS–PVP block copolymer micelle is shielded from the surrounding homopolymer by the corona, so that micelles behave in some ways as if they were very high molecular weight dPS polymers. The isotopic effect therefore gives rise to a tendency for these micelles to segregate to the free surface.

The arguments presented above can be applied to any preexisting interface. In general, there will be two such interfaces: the interfacial block copolymer layer and the surface segregated layer. The tendency for micelles to segregate to these layers depends on the detailed shapes of the dPS profiles within the micelles and within the segregated layers. With these ideas in mind, the results presented in Figure 6 can be understood in terms of the differing behaviors of individual chains and micelles. The segregation of free chains to the PS–PVP interface is uniquely determined by μ_c, which rises rapidly with the copolymer concentration until ϕ_{cmc}^{ps} is reached, at which point it remains fixed at μ_{cmc}^{ps}. The formation of micelles is therefore associated with a plateau in the interface segregation of the free chains and by the onset of surface segregation of the micelles themselves. Inspection of parts a and b of Figure 6 indicates that this transition occurs at copolymer volume fractions of 4.5% for the 391–68 copolymer and 1% for the 355–125 copolymer. The 391–68 copolymer exhibits a sharp increase in the interface segregation for copolymer concentrations greater than ϕ_{cmc}^{ps}, which we attribute to the preferential segregation of micelles to the interfacial layer.

Comparison to Mean-Field Theory

A mean-field theory can be used to describe the phase behavior and interfacial properties of the PS homopolymer/PVP homopolymer/dPS–PVP diblock copolymer system. We begin with an expression for the free energy density of a homogeneous mixture in terms of the volume fractions of the different components. The volume fractions of the individual copolymer blocks are $\phi_{c\text{-}dps}$ for the dPS block and $\phi_{c\text{-}pvp}$ for the PVP block. The volume fractions of the PS and PVP homopolymers are $\phi_{h\text{-}ps}$ and $\phi_{h\text{-}pvp}$, respectively. It is helpful to define the quantity ϕ_{ps}, which is the overall volume fraction of PS (or dPS) segments, given by $\phi_{ps} = \phi_{c\text{-}dps} + \phi_{h\text{-}ps}$. A similar quantity, ϕ_{pvp}, is defined such that $\phi_{pvp} = \phi_{c\text{-}pvp} + \phi_{h\text{-}pvp}$. The zero free energy state is a hypothetical unmixed state in which there is no interaction between copolymer blocks. The free energy density, f, can be written in terms of three χ parameters, which describe the thermodynamic interactions between the three different segment types

$$\frac{f}{\rho_0 k_B T} = \frac{\phi_{h\text{-}ps} \ln \phi_{h\text{-}ps}}{N_{h\text{-}ps}} + \frac{\phi_{h\text{-}pvp} \ln \phi_{h\text{-}pvp}}{N_{h\text{-}pvp}} + \frac{\phi_c \ln \phi_c}{N_c} + \chi_{ps\text{-}pvp}\phi_{h\text{-}ps}\phi_{pvp} + \chi_{dps\text{-}pvp}\phi_{c\text{-}dps}\phi_{pvp} + \chi_{dps\text{-}ps}\phi_{c\text{-}dps}\phi_{h\text{-}ps} \quad (4)$$

where ρ_0 is the segment concentration and N_c is the total block copolymer degree of polymerization, given by $N_c = N_{c\text{-}dps} + N_{c\text{-}pvp}$. The value of $\chi_{dps\text{-}ps}$ is approximately 10^{-4},[15] whereas the value of $\chi_{ps\text{-}pvp}$ is approximately 0.1 as determined from our results and from consideration of the heat of mixing data for small-molecule analogues of PS and PVP as described in Appendix 2. Contributions to $\chi_{dps\text{-}pvp}$ arising from the isotopic interaction between the normal PVP segments and the deuterated dPS segments are expected to be of the same order as $\chi_{dps\text{-}ps}$. The most important interactions are between PS and PVP segments, and these interactions are essentially independent of whether or not the PS is deuterated. When the PS–PVP interactions are shielded, the small dPS–PS interaction may be dominant, as mentioned previously with regard to the segregation of dPS–PVP block copolymer micelles. We can neglect these small interactions when considering individual polymer chains at the PS–PVP interface, and here we make the approximations $\chi_{ps\text{-}pvp} = \chi_{dps\text{-}pvp}$, $\chi_{dps\text{-}ps} = 0$ to obtain the following relation for

the free energy density:

$$\frac{f}{\rho_0 k_B T} = \frac{\phi_{h\text{-}ps} \ln \phi_{h\text{-}ps}}{N_{h\text{-}ps}} + \frac{\phi_{h\text{-}pvp} \ln \phi_{h\text{-}pvp}}{N_{h\text{-}pvp}} + \frac{\phi_c \ln \phi_c}{N_c} + \chi_{ps\text{-}pvp}\phi_{ps}\phi_{pvp} \quad (5)$$

The copolymer chemical potential is given as follows:[16]

$$\frac{\mu_c}{N_c} = \frac{\partial(f/\rho_0)}{\partial\phi_k} + f/\rho_0 - \sum_{k=c,ps,pvp} \phi_k \frac{\partial(f/\rho_0)}{\partial\phi_k} \quad (6)$$

By making the further assumption that $\chi_{ps\text{-}pvp}$ is not a function of the volume fractions, we arrive at the following for μ_c:

$$\frac{\mu_c}{k_B T} = \ln \phi_c + 1 - N_c K_\phi + \chi_{ps\text{-}pvp}\{N_{c\text{-}dps}\phi_{pvp}^2 + N_{c\text{-}pvp}\phi_{ps}^2\} \quad (7)$$

with $K_\phi = \phi_{h\text{-}ps}/N_{h\text{-}ps} + \phi_{h\text{-}pvp}/N_{h\text{-}pvp} + \phi_c/N_c$. The relevant volume fractions in the bulk PS phase are ϕ_c^{ps}, ϕ_{pvp}^{ps}, and ϕ_{ps}^{ps}. When the bulk PS phase consists of nearly pure homopolymer, i.e., $\phi_c^{ps} \ll 1$, $\phi_{pvp}^{ps} \ll 1$, and $\phi_{ps}^{ps} \approx 1$, eq 7 can be rewritten to give the following for ϕ_c^{ps}:

$$\phi_c^{ps} = \exp\left\{\frac{\mu_c}{k_B T} - 1 + \frac{N_c}{N_{h\text{-}ps}} - \chi_{ps\text{-}pvp}N_{c\text{-}pvp}\right\} \quad (8)$$

Equation 8 was derived from the assumption that the polymers mix uniformly and is therefore valid only when micelles are not present. When micelles are present, eq 8 gives the volume fraction of free block copolymer chains in the PS phase. The mobility of block copolymer micelles in high molecular weight matrices is exceptionally low, and the transfer of copolymer chains across the PS layer is governed by the motion of the free block copolymer chains. The relatively weak dependence of the mobility of these free block copolymer chains on the chain degree of polymerization ($\propto N_c^{-2}$ for reptation) cannot explain the dramatic increases in the equilibration times with increasing $N_{c\text{-}pvp}$. Rather, it is the much stronger, exponential dependence of the concentration of free copolymer chains on $N_{c\text{-}pvp}$ that is responsible for the slowing down of the equilibration process.

A description of the length scale of a polymer chain must also be included if interfacial properties are to be understood. Polymer chains in the melt obey Gaussian statistics, so that a single parameter can be used to characterize this length scale. The most convenient parameter is the statistical segment length, a, defined as

$$a^2 = \langle R^2 \rangle / N \quad (9)$$

where $\langle R^2 \rangle$ is the mean-squared end-to-end distance of a polymer chain and N is its degree of polymerization. Neutron-scattering measurements have given 6.7 Å as the statistical segment length for PS.[17] The chain dimensions of PS and PVP in Θ solvents are nearly identical,[18] and we therefore assume that the statistical segment length for PVP is also 6.7 Å. We also assume that PVP has the same segment concentration as PS, i.e., 9.40×10^{-3} mol/cm^3 at 178 °C.[19]

The compositions of the bulk phases and the interfacial properties are completely specified by μ_c, $\chi_{ps\text{-}pvp}$, a, and the molecular weights of the polymeric components. The profiles of the different polymer components across the interface, and the interfacial tension, are determined by solving a set of modified diffusion equations for various polymer chain probability distribution functions in mean fields that are themselves functions of the local composition. The mean fields are obtained by expressing the local free energy density in the form of eq 5, with the requirement that the density remains constant across the interface. The procedure is described in detail in the accompanying publication.[4]

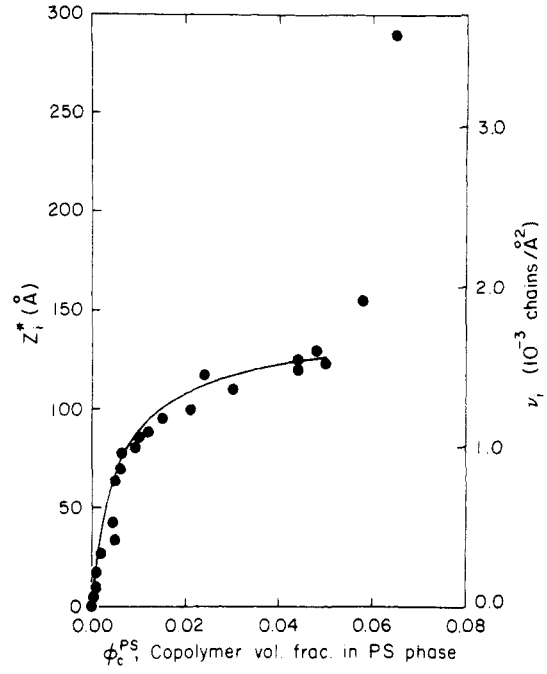

Figure 8. Interface copolymer excess for the 391–68 copolymer as a function of copolymer volume fraction in the PS phase: measured values (●), and predictions from the mean-field theory, assuming $\chi_{ps\text{-}pvp} = 0.11$ (—).

We use $\chi_{ps\text{-}pvp}$ as an adjustable parameter in order to obtain a good fit to the concentration dependence of z_i^* for the 391–68 copolymer. The experimental data are replotted in Figure 8, along with a theoretical curve obtained by assuming $\chi_{ps\text{-}pvp} = 0.11$. The concentration dependence of the surface tension as derived from the mean-field theory with $\chi_{ps\text{-}pvp} = 0.11$ is plotted in Figure 9. The theory gives 3.04 dyn/cm for γ_0, the interfacial tension in the absence of block copolymer. The mean-field value of γ_0 in the limit of infinite homopolymer molecular weight is given by[20]

$$\gamma_0^\infty = a\rho_0 k_B T(\chi/6)^{1/2} \quad (10)$$

Equation 10 gives 3.20 dyn/cm for this infinite molecular weight limit, indicating that corrections to γ_0 associated with the finite homopolymer molecular weights are small.

Polydispersity of the PVP block length can complicate the interpretation of the concentration-dependent data because of the very strong dependence of ϕ_c^{ps} on the product $\chi_{ps\text{-}pvp}N_{c\text{-}pvp}$. Polydispersity corrections may explain why the concentration dependence for the interfacial segregation of the 355–125 copolymer cannot also be fit by using $\chi_{ps\text{-}pvp} = 0.11$. A copolymer chemical potential of $5.5k_BT$ gives a predicted z_i^* of 137 Å for the 355–125 copolymer, which within experimental error is the measured plateau value assumed to be associated with the presence of micelles. The corresponding ϕ_{cmc}^{ps} from eq 8 is 0.1%. The actual plateau in the interfacial segregation is not reached until the copolymer concentration in the PS phase reaches 1%, for which eq 8 gives $\chi_{ps\text{-}pvp}N_{c\text{-}pvp} = 9.2$, as compared to $\chi_{ps\text{-}pvp}N_{c\text{-}pvp} = 13.8$ for $\chi_{ps\text{-}pvp} = 0.11$. The 1% block copolymer in the PS phase at the micelle transition may therefore consist of molecules with lower PVP block lengths than the number-average value of 125. The 355–125 copolymer is more sensitive to variations in $N_{c\text{-}pvp}$ simply because ϕ_{cmc}^{ps} is lower than it is for the 391–68 copolymer, and it is for this reason that we have used

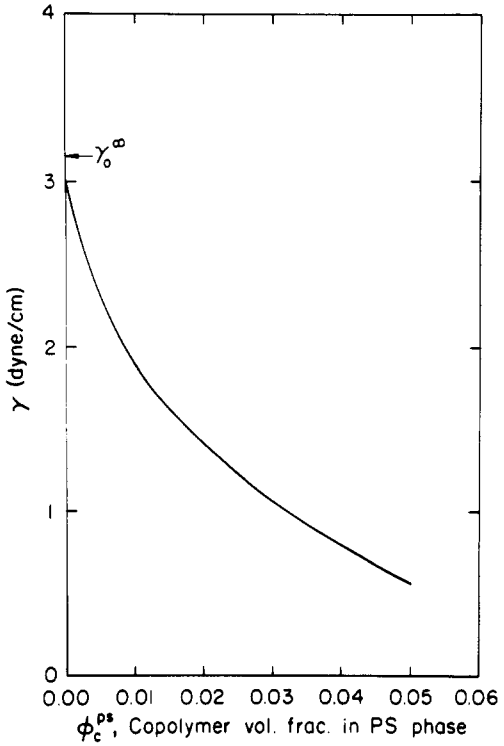

Figure 9. Interfacial tension, as determined by the mean-field theory with $\chi_{ps\text{-}pvp} = 0.11$, as a function of the volume fraction of the 391–68 copolymer in the PS phase.

Table II
Values of μ_{cmc}^{ps} As Derived from z_i^* and As Predicted by the Simplified Theory of Micelle Formation with $\chi = 0.11$

block copolymer	z_i^* at cmc (measd), Å	μ_{cmc}^{ps}/k_BT from z_i^*	μ_{cmc}^{ps}/k_BT micelle theory
391–68	126 ± 13	5.25 ± 0.5	3.5
355–125	137 ± 14	5.5 ± 0.5	4.1
1300–173	210 (estimate)	≈5.5	4.9

the interfacial segregation behavior of the 391–68 copolymer for our determination of $\chi_{ps\text{-}pvp}$.

The theoretical relationship between z_i^* and μ_c is only weakly dependent on the quantity $\chi_{ps\text{-}pvp}N_{c\text{-}pvp}$. For this reason μ_{cmc}^{ps} is a more meaningful parameter than ϕ_c^{ps}. Measurements of z_i^* in the regime where micelles are present but do not segregate to the interface can be used to determine μ_{cmc}^{ps} by comparison to the theoretical relationship between z_i^* and μ_c. The results of such a comparison for the three copolymers used in this study are listed in Table II, where we have assumed a 10% accuracy in the measurement of the relevant z_i^*. Predictions from a simple model of micelle formation, outlined in Appendix 1, are also listed in Table II. The copolymer chemical potentials derived from the segregation results are higher than the values obtained from the theory of micelle formation. We attribute this discrepancy to the fact that the simplified theory neglects certain contributions to the micellar free energy that may in fact be significant.

We have used the mean-field theory to obtain the relationship between z_i^* and μ_c. As described in ref 4, the theory can be used to extract much more detailed information, including the interfacial tension and concentration profiles for any of the molecular components. The calculated values of the interfacial tension at μ_{cmc} are included in Table III. These calculated values of γ represent significant decreases from γ_0, as was shown in Figure 9 for the 391–68 copolymer. Calculated profiles for the dPS and PVP blocks of the three copolymers at the

Table III
Values of the Interfacial Tension at μ_{cmc}^{ps} As Calculated by the Mean-Field Theory with $\chi_{ps\text{-}pvp} = 0.11$ ($\gamma_0 = 3.04$ dyn/cm)

block copolymer	μ_{cmc}/k_BT (from z_i^*)	γ, dyn/cm
391–68	5.25 ± 0.5	0.56 ± 0.5
355–125	5.5 ± 0.5	0.56 ± 0.5
1300–173	≈5.5	≈1.1

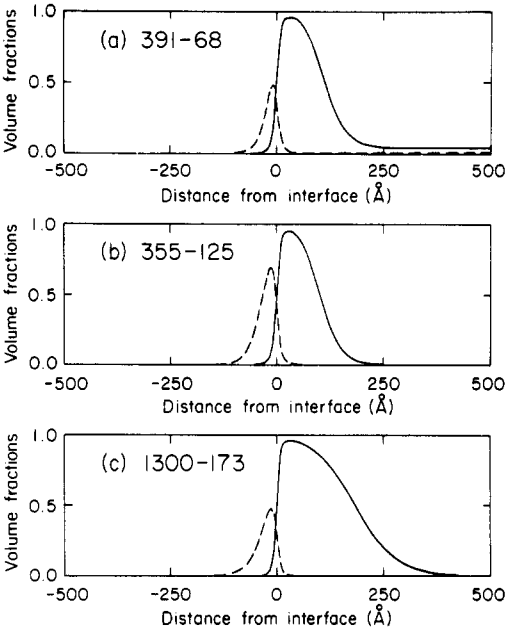

Figure 10. Calculated concentration profiles for the dPS block (—) and the PVP block (- - -) for the three copolymers at the experimentally determined values of μ_{cmc}: (a) 391–68 copolymer, $\mu_{cmc} = 5.25k_BT$, $z_i^* = 126$ Å, (b) 355–125 copolymer, $\mu_{cmc} = 5.5k_BT$, $z_i^* = 137$ Å, (c) 1300–173 copolymer, $\mu_{cmc} = 5.5k_BT$, $z_i^* = 210$ Å.

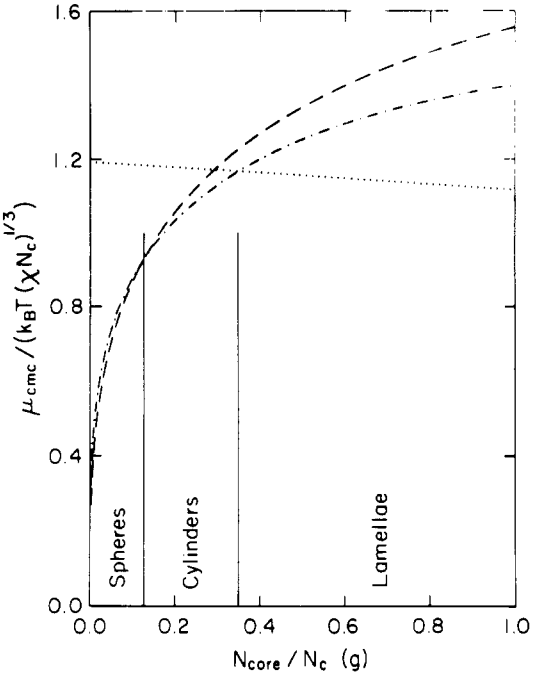

Figure 11. Dependence of μ_{cmc} on the copolymer asymmetry as derived from the simplified theory of micelle formation for spheres (—), cylinders (- - -), and lamellae (· · ·). The predicted regions of stability for each micelle geometry are indicated.

experimentally determined values of μ_{cmc}^{ps} are shown in Figure 10. In each case there is a region at the interface where the dPS block volume fraction is nearly unity. This layer is the deuterated polystyrene layer mentioned earlier toward which micelles have a tendency to segregate.

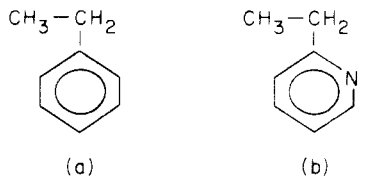

Figure 12. Chemical structures of small-molecule analogues for PS and PVP: (a) ethylbenzene, (b) 2-ethylpyridine.

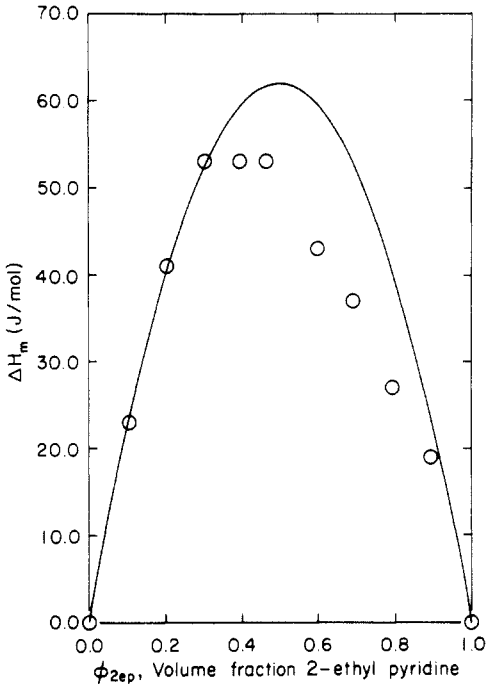

Figure 13. Heat of mixing data from ref 26 for ethylbenzene and 2-ethylpyridine at 25 °C, as a function of the volume fraction of 2-ethylpyridine. The solid line is a fit to the regular solution form, $\Delta H_m = RT\chi\phi_{2ep}(1 - \phi_{2ep})$, with $\chi = 0.1$.

Conclusions

The interfacial activity of diblock copolymer chains at homopolymer interfaces can be understood quantitatively in terms of a mean-field theory. The following general conclusions relate to the work described here:

1. The equilibrium segregation of block copolymers to an interface between homopolymers is a function of the copolymer chemical potential. This chemical potential is generally limited by the formation of copolymer micelles in the homopolymer phases.

2. Equilibration between the interface and a micellar phase is directly affected by the solubility of individual copolymer chains and can be a very slow process. For this reason, measurements of the interfacial block copolymer excess are often a better probe of the equilibrium interfacial properties than are direct measurements of the interfacial tension.

3. There is a tendency for dPS–PVP block copolymer micelles in the PS phase to segregate to existing interfaces. Driving forces for this type of segregation arise from enthalpic interactions between PS and dPS and from entropic contributions to the free energy associated with constraints imposed on high molecular weight polymers at sharp interfaces.

4. The copolymer chemical potential at the micelle transition can be determined from a proper interpretation of measurements of the interfacial copolymer segregation, taking into account the possibility of interfacial segregation of block copolymer micelles. This technique is particularly useful when the critical micelle concentration is too low to be measured directly.

Acknowledgment. This work was supported by the NSF–DMR Materials Program through the Cornell Materials Science Center. K.R.S is grateful to AT&T for support in the form of a Ph.D. fellowship. We also thank Markus Antonietti for supplying the high molecular weight PVP homopolymer and Richard Jones for many helpful discussions.

Appendix 1: Theory of Micelle Formation

Here we present a simple model of the micelle transition in order to obtain an estimate of μ_{cmc}. The model was initially developed by Leibler for spherical micelles[21] and is extended here to include cylindrical and lamellar micelles as well. Model calculations[22] and experimental results[23] have indicated that these alternate micellar geometries exist.

A micelle consists of an interior core region, an external corona region in contact with the homopolymer matrix, and an interfacial region, which separates the core and corona. We assume that the interfacial region is narrow in comparison to the core and corona widths, in which case the micellar free energy can be written as a sum of components from each region:

$$F_{micelle} = F_{interface} + F_{core} + F_{corona} \qquad \text{(A-1)}$$

The interfacial free energy is approximated by the form for infinite molecular weight homopolymers

$$F_{interface}/k_BT = Aa\rho_0(\chi/6)^{1/2} \qquad \text{(A-2)}$$

where A is the interfacial area separating the core and the corona. The core and corona free energies arise from the loss of configurational entropy of the block copolymer in these regions. The free energy of the core can be written in the form

$$F_{core}/k_BT = QK(R_{core}^2/N_{core}a^2) \qquad \text{(A-3)}$$

where Q is the number of chains per micelle, N_{core} is the degree of polymerization of the core block of the copolymer, and K is a constant that depends on the micellar geometry. For lamellar micelles R_{core} is defined as half the thickness of the inner lamella. Semenov has calculated $K = 0.370$ for spheres, $K = 0.616$ for cylinders, and $K = 1.234$ for lamellae.[24] An expression for the corona energy is obtained by assuming that the corona is not swollen by the solvent homopolymer chains, a valid assumption when the homopolymer molecular weight is very high. The corona free energy is obtained from the expression for the free energy of a continuously stretched chain[25]

$$\frac{F_{corona}}{k_BT} = \frac{3Q}{2a^2}\int_{r=R_{core}}^{r=R} dr\left(\frac{dr}{dn}\right) \qquad \text{(A-4)}$$

where the index n runs from 0 at one end of the corona block to N_{corona} at the other end of the corona block and R is the overall radius of the micelle.

The chemical potential of copolymer chains in the presence of micelles is given by $\mu_c = \delta F_{micelle}/\delta Q$. A transition from a homogeneous phase to a micellar phase occurs when the excess free energy associated with the micelles is zero, i.e., $F_{micelle} - Q\mu_{cmc} = 0$. The condition that $\delta F_{micelle}/\delta Q = F_{micelle}/Q$ requires that $\delta(F_{micelle}/Q)/\delta Q = 0$. The copolymer chemical potential at the micelle transition is therefore given by $F_{micelle}(Q^*)/Q^*$, where Q^* is the value of Q for which $\delta(F_{micelle}/Q)/\delta Q = 0$.

Spherical Micelles. For spherical micelles $F_{micelle}/Q$ can be written entirely in terms of Q, by using the following

relationships:

$$(4/3)\pi R_{core}^3 = QN_{core}/\rho_0, \quad (4/3)\pi R^3 = QN_c/\rho_0 \tag{A-5}$$

$$A = 4\pi R_{core}^2 \tag{A-6}$$

$$4\pi r^2\, dr = Q\, dn/\rho_0 \tag{A-7}$$

Evaluation of $F_{micelle}/Q$ at its minimum value gives the following for the chemical potential at which spherical micelles will form, as given by Leibler:[21]

$$\mu_{cmc}^{spheres}/k_BT = 1.72(\chi N_c)^{1/3}g^{4/9}(1.74g^{-1/3} - 1)^{1/3} \tag{A-8}$$

Here g is equal to N_{core}/N_c and represents the asymmetry of the block copolymer chains.

Cylindrical Micelles. A similar analysis can be made for cylindrical micelles. Here $F_{micelle}/Q$ is written entirely in terms of R_{core} with the aid of the relations

$$\pi R_{core}^2 L = QN_{core}/\rho_0, \quad \pi R^2 L = QN_c/\rho_0 \tag{A-9}$$

$$A = 2\pi R_{core} L \tag{A-10}$$

$$2\pi r L\, dr = Q\, dn/\rho_0 \tag{A-11}$$

where L is the length of cylindrical micelle. Minimization of $F_{micelle}/Q$ with respect to R_{core} is equivalent to minimization of $F_{micelle}/Q$ with respect to Q. Evaluation of $F_{micelle}/Q$ at the minimum with respect to R_{core} gives

$$\mu_{cmc}^{cylinders}/k_BT = 1.19(\chi N_c)^{1/3}g^{1/3}(1.64 - \ln g)^{1/3} \tag{A-12}$$

Lamellar Micelles. The following relationships are used to write $F_{micelle}/Q$ for lamellar micelles in terms of R_{core}:

$$AR_{core} = QN_{core}/\rho_0, \quad AR = QN_c/\rho_0 \tag{A-13}$$

$$A\, dr = Q\, dn/\rho_0 \tag{A-14}$$

Evaluation of $F_{micelle}/Q$ at the minimum with respect to R_{core} gives

$$\mu_{cmc}^{lamellae}/k_BT = 0.67(\chi N_c)^{1/3}(5.64 - g)^{1/3} \tag{A-15}$$

Comparison of the Geometries. The values of μ_{cmc} obtained for each micellar geometry are plotted as functions of g in Figure 11. The preferred micellar geometry is the one that appears at the lowest copolymer chemical potential. Comparison of eqs A-8, A-12, and A-15 indicates that within the approximations made here the micelles are expected to be spherical for $g < 0.13$, cylindrical for $0.13 < g < 0.35$, and lamellar for $g > 0.35$. These three regions of stability are indicated in Figure 11. The result that the preferred geometry depends only on the copolymer composition arises from the assumption that the matrix homopolymer chains do not swell the micelle corona. Swelling of the corona gives a lower effective g and can significantly affect the results.

Some contributions to the micellar free energy have been left out of eq A-1 so that an analytic expression for μ_{cmc} could be derived. One such contribution involves end corrections to the interfacial term associated with the localization of block copolymer joints in a narrow region at the center of the interface.[4,24] An additional contribution arises from the entropy loss of high molecular weight homopolymer chains at the homopolymer–corona interface.[4] Inclusion of these correction terms will give a higher value of μ_{cmc}. Differences in the copolymer chemical potential for different structures are often quite small, and even small corrections to the micelle free energy expressions can have a dramatic effect on the calculated stability regions. As a result it is much easier to obtain an estimate for μ_{cmc} than it is to predict which type of micellar structure will actually appear. Nevertheless, the simplified theory gives a basis for the more general conclusion that μ_{cmc} is lower when the shorter block forms the core, since structures can be formed that distort the copolymer chains to a lesser degree. We use the derivation presented above as a simple approximation to μ_{cmc}, which is most useful when very high molecular weight homopolymer chains are the solvent for the copolymer.

Appendix 2: Estimation of $\chi_{ps\text{-}pvp}$

An estimate of the magnitude of $\chi_{ps\text{-}pvp}$ can be obtained by considering heat of mixing data for mixtures of ethylbenzene and 2-ethylpyridine. These are the closest small-molecule analogues of PS and PVP, as illustrated by the chemical structures shown in Figure 12. In Figure 13 heat of mixing data from the literature[26] is plotted as a function of ϕ_{2ep}, the volume fraction of 2-ethylpyridine. The solid line is a fit to the regular solution form

$$\Delta H_m = RT\chi\phi_{2ep}(1 - \phi_{2ep}) \tag{A-16}$$

with $\chi = 0.1$. The χ parameter defined by eq A-16 is equal to $\chi_{ps\text{-}pvp}$ as defined by eq 4 if the entropy of mixing of ethylbenzene and 2-ethylpyridine is ideal. However, this small-molecule χ parameter corresponds to a degree of polymerization of 1 and a temperature of 25 °C. The effect of temperature and chain length on the χ parameter are poorly understood, and the value of 0.1 for $\chi_{ps\text{-}pvp}$ is merely an estimate of its value for high molecular weight polymers at 178 °C.

References and Notes

(1) Yee, A. F. *Encycl. Polm. Sci. Eng.* **1986**, *8*, 1.
(2) Gaillard, P.; Ossenbach-Sauter, M.; Reiss, G. *Makromol. Chem., Rapid Commun.* **1980**, *1*, 771.
(3) Anastasiadis, S. H.; Gancarz, I.; Koberstein, J. T. *Macromolecules* **1989**, *22*, 1449.
(4) Shull, K. R.; Kramer, E. J. *Macromolecules*, previous paper in this issue.
(5) Brown, H. R. *Macromolecules* **1989**, *22*, 2859.
(6) Creton, C.; Hui, H. C. Y.; Kramer, E. J.; Hadziioannou, G.; Brown, H. R. *Bull. Am. Phys. Soc.* **1989**, *34*, 709.
(7) Fayt, R.; Jerome, R.; Teyssié, Ph. *J. Polym. Sci., Polym. Phys. Ed.* **1982**, *20*, 2209.
(8) Fayt, R.; Jerome, R.; Teyssié, Ph. *Polym. Eng. Sci.* **1987**, *27*, 328.
(9) Green, P. F.; Mills, P. J.; Palmstrøm, C. J.; Mayer, J. W.; Kramer, E. J. *Phys. Rev. Lett.* **1984**, *53*, 2145.
(10) Mills, P. J.; Green, P. F.; Palmstrøm, C. J.; Mayer, J. W.; Kramer, E. J. *Appl. Phys. Lett.* **1984**, *45*, 957.
(11) Green, P. F.; Mills, P. J.; Kramer, E. J. *Polymer* **1986**, *27*, 1063.
(12) Leibler, L.; Orland, H.; Wheeler, J. C. *J. Chem. Phys.* **1983**, *79*, 3550.
(13) Bartell, L. S.; Roskos, R. R. *J. Chem. Phys.* **1966**, *44*, 457.
(14) Jones, R. A. L.; Kramer, E. J.; Rafailovich, M. H.; Sokolov, J.; Schwarz, S. A. *Phys. Rev. Lett.* **1989**, *62*, 280.
(15) Bates, F. S. *Macromolecules* **1986**, *19*, 793.
(16) Sanchez, I. C. *Encycl. Polym. Sci. Technol.* **1987**, *11*, 1.
(17) Tangari, C.; King, J. S.; Summerfield, G. C. *Macromolecules* **1982**, *15*, 132.
(18) *Polymer Handbook*, 2nd ed.; Wiley: New York, 1975.
(19) Hellmege, K.; Knappe, W.; Lehmann, P. *Kolloid-Z.* **1963**, *183*, 110.
(20) Helfand, E.; Tagami, Y. *Polym. Lett.* **1971**, *9*, 741.
(21) Leibler, L. *Makromol. Chem., Macromol. Symp.* **1988**, *16*, 1.
(22) Mayes, A. M.; Olvera de la Cruz, M. *Macromolecules* **1988**, *21*, 2543.
(23) Kinning, D. J.; Winey, K. I.; Thomas, E. L. *Macromolecules* **1988**, *21*, 3502.
(24) Semenov, A. N. *Sov. Phys.-JETP* **1985**, *61*, 733.
(25) de Gennes, P.-G. *Scaling Concepts in Polymer Physics*; Cornell University Press: Ithaca, NY, 1979.
(26) Woyicki, W. *J. Chem. Thermodyn.* **1972**, *4*, 1.